Advanced Materials Science and Technology Vol 5 Issue 1 2023
DOI: 10.37155/2717–526X–0501–7

ORIGINAL RESEARCH ARTICLE

Open Access

Omniscient Pte.Ltd.

The Thermal Kinetics of Methanol Oxidation on Pt/MWCNT Electrocatalysts in Alkaline Media

Haitao Zheng* and Mmalewane Modibedi

Energy Centre, Council for Scientific and Industrial Research (CSIR), POBOX 395, Pretoria 0001, South Africa.

***Correspondence to:** Haitao Zheng, Energy Centre, Council for Scientific and Industrial Research (CSIR), PO Box 395, Pretoria 0001, South Africa. Email: hzheng@csir.co.za

Received: August 24, 2023; **Accepted:** September 28, 2023; **Published Online:** September 30, 2023

Citation: Zheng H and Modibedi M. The Thermal Kinetics of Methanol Oxidation on Pt/MWCNT Electrocatalysts in Alkaline Media. *Advanced Materials Science and Technology*, 2023;5(1):0521211. https://doi.org/10.37155/2717-526X-0501-7

Abstract: In this study, the thermal electrooxidation of methanol on a Pt/MWCNT catalyst was examined in alkaline media across the temperature range of 298-363 K. The investigation utilized cyclic voltammetry (CV), quasi-state polarization, and electrochemical impedance spectroscopy (EIS) methods to explore the kinetics of the methanol electrooxidation reaction (MEOR). At elevated temperatures, the kinetics of methanol electro-oxidation on the Pt/MWCNT catalyst within an alkaline solution (1.0 mol/L KOH) were notably accelerated compared to room temperature. This acceleration can be attributed to the reduced methanol dehydrogenation reaction at relatively low temperatures. The Tafel slopes experienced changes as the temperature increased. These variations in Tafel slopes are likely linked to alterations in the rate-determining step of the MEOR as a function of temperature. The EIS outcomes revealed a decrease in charge-transfer resistance as temperature increased. This phenomenon is associated with the interplay between interfacial and diffusion impedances, as well as the surface roughness of the highly dispersed electrode surface.

Keywords: Electro-oxidation of methanol; Pd/MWCNT; Catalyst; Alkaline media; Temperature

1. Introduction

The methanol electrooxidation reaction (MEOR) in acid media has been extensively investigated as an anodic reaction in direct methanol fuel cells[1-3], and often represented by the general dual path mechanism[4]. In acidic environments, the electrooxidation of methanol generates CO-like poisoning intermediates that absorb onto the Pt active sites on the catalyst surface. This phenomenon leads to a pronounced limitation in oxidation kinetics, resulting in substantial polarization losses[5,6]. Moreover, the rate of methanol permeation in proton exchange membrane fuel cells (PEMFCs) is notably high due to the electro-osmotic drag

associated with the proton conduction mechanism. However, when direct methanol fuel cells (DMFCs) operate in alkaline media, the kinetics of the MEOR experience significant enhancement, enabling the use of more cost-effective catalysts[5-9]. In this context, the MEOR kinetics on Pt/C and Pt-Ru/C catalysts are evaluated at 295 K and 333 K, using solution of 0.5 mol/L H_2SO_4 and 0.1 mol/L NaOH. Notably, the kinetics of Pt and Pt-Ru for MEOR were found to be substantially faster in an alkaline solution compared to an acid solution[10].

The electrocatalytic activity of metal nanoparticles is widely acknowledged to be greatly influenced by factors such as their support, shape, size, and dispersion[11-13]. Over the past decades, there has been extensive research into the use of carbon nanotubes as a support material for Pt-based catalysts in direct methanol fuel cells (DMFCs). This choice is motivated by the substantial surface area, excellent conductivity, and remarkable chemical stability offered by carbon nanotubes[14]. Notably, catalysts supported on multiwall carbon nanotube (MWNT) have demonstrated superior performance in DMFCs compared to carbon black (XC-72), both in half-cell characterization and full cell performance test, conducted under identical conditions[15-17].

A swift synthesis approach employing microwave irradiation technique (MIT) has been introduced for the fabrication of Pt catalyst supported on both carbon and carbon nanotube. This method yields a uniform Pt catalyst supported on carbon with particle size below 5nm. Electrochemical assessments demonstrated that Pt/C and Pt/MWCNT catalysts produced by the MIT technique, displayed notably increased electrochemically active area and enhanced catalytic activity for the methanol electro-oxidation reaction in acid solution, surpassing the performance of a commercial Pt/C catalyst[18-21].

To our understanding, a comprehensive investigation into the impact of temperature on the kinetics of methanol electrooxidation reaction (MEOR) on Pt/MWCNT catalysts within an alkaline solution has not been extensively documented. The objective of this study was to provide a deeper insight into how temperature influences the MEOR over Pt/MWCNT catalysts within an alkaline environment.

2. Experimental

2.1 Pretreatment of the Carbon Nanotube

The pretreatment of MWCNTs (Shenzhen Nanotech. Co., Ltd., China) using a mixture of 98% H_2SO_4 and 65% HNO_3 (1:1 by volume) was stirred for 15 min and then refluxed at 140 ^oC for 4 hours. The acid pretreated MWCNTs were thoroughly rinsed with distilled deionized water until neutral and dried at 80 ^oC for 24 h.

2.2 Synthesis of the Electrocatalysts

Pt supported on MWCNT was synthesized by the microwave irritation technique (MIT). The pretreated MWCNT (50 mg) was mixed with 10 mL of 2-propanol under ultrasonic treatment for 20 min, then 5.4 mL of H_2PtCl_6 solution (1.85 mg/mL Pt^{2+}) was slowly added to the MWCNT dispersion, followed by ultrasonic treatment for 30 min. then evaporation of the solvent using a domestic microwave oven. The procedure was 5s of irradiation on and 60 s of irradiation off for six times. The resulting sample was dispersed in formic acid (10 mL, 1.0 mol/L HCOOH) and then purged under argon for 15 min to remove oxygen. The oxygen-free solution was heated under an argon atmosphere in a 20 s irradiation on and 60 s irradiation off until the sample was completely dried. The Pt loading in MWCNT was kept as ~20 wt%. The Pt content was determined by ICP-AES.

2.3 Preparation of the Electrodes

1.0 mg of 20 wt% Pt/MWCNT powders was dispersed in 2.0 mL 2-propanol with 5 wt% Nafion solution (DuPont, USA) (2-propanol: Nafion = 20:1) under ultrasonic stirring. The ink of well-mixed catalysts was then deposited on the surface of glass carbon with a diameter of 2.0 mm. Pt loadings on each electrode were normally controlled at ~ 0.2 mg/cm^2.

2.4 Electrochemistry Measurements

The experiments were carried out in a standard three-electrode cell controlled at room temperature. Electrochemical experiments were performed with AUTOLAB. A platinum foil (2.0 cm^2) and Hg/HgO (1.0 mol/dm^3) were used as counter and reference electrodes, respectively. The frequencies for the impedance test range from 100 KHz to 0.1 Hz. The temperature controlled by an oil bath with a thermal regulator.

2.5 Characterization of the Catalysts

2.5.1 X-ray diffraction (XRD)

X-ray diffraction (XRD) was employed to obtain the information on the surface and bulk structure of the catalyst and was carried out with a D/MAX2200 diffract meter employing CuK radiation (λ = 0.15418 nm).

2.5.2 Transmission electron microscopic (TEM) measurement

Transmission electron microscopic (TEM) images were generated with a Philips CM-300 high-resolution system operating at 200 keV.

3. Results and Discussion

3.1 XRD and TEM Analysis

Figure 1 presents the XRD pattern and TEM image of Pt/MWCNTS catalysts, the XRD pattern **(Figure 1a)** distinctly displays the five prominent characteristic peaks corresponding to the Pt face-centered cubic structure. These planes are [111], [200], [220], [311] and [222], respectively, signifying the f.c.c. crystal structure. Additionally, the peak observed at ca.2θ = 26º is attributed to graphite, indicating the graphitic structure of the carbon nanotube. The estimated average size of the Pt/MWCNTS nanoparticles was determined utilizing Scherrer's equation $d = 0.89\lambda/B\cos\theta$, where d represents the average particle diameter, λ denotes the wavelength of X-ray radiation (0.154056 nm), θ signifies the angle of the peak (220), and B indicates the width in radians of the diffraction peak at half height. The calculated average particle size of Pt/MWCNTS is 5.5 nm.

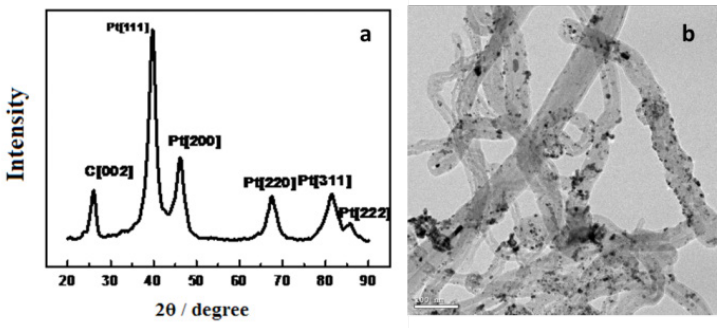

Figure 1. XRD patterns (a) and TEM image (b) of Pt/MWCNT catalyst

Figure 1b exhibits typical TEM image of Pt/MWCNTS catalysts. Within this image, the Pt particles are observed to be dispersed with a size distribution spanning from 3.3 nm to 6 nm on the MWCNTs, the mean size of the Pt nanoparticle was estimated to be approximately 5 nm.

3.2 Electrochemistry Performance

Figure 2 illustrates the cyclic voltammogram (CV) obtained from the Pt/MWCNT catalysts, recorded in alkaline solutions (1.0 mol/L KOH). The shape of CV curve on the Pt/MWCNT catalysts shows a typic curve of Pt electrode. Two symmetric peaks are attributed to the occurrence of the hydrogen absorption reaction in the -0.8 V to -0.5 V region. At a positive potential, a small PtO peak starts to form at -0.1 V on the surface and the corresponding current plateau continues up to a potential of 0.3 V. The electrochemical surface area (ECSA) is a critical parameter used to assess the performance of an electrocatalyst. It provides insights into the active surface area available for electrochemical reactions. The ECSA was calculated by integrating the charges associated with the peak from reduction of Pt between -0.80 V ~ -0.5 V[22]. The approximate value of the ECSA on the Pt/MWCNT electrode is 31.2 m^2/g^2.

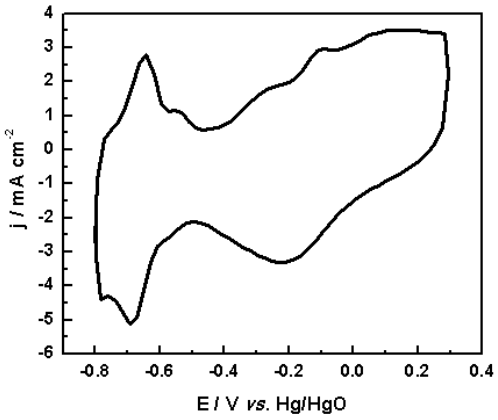

Figure 2. Cyclic voltammogram in alkaline (1 mol/L KOH) at 298 K on Pt/MWCNT electrode

The exchange current density is an important parameter in electrochemistry, which derived from Tafel plot and can be determined experimentally by extrapolating the linear Tafel lines, which relate the overpotential to the logarithm of the current density, to the point where the overpotential equals zero. **Table 1** provides a comprehensive overview of the electrochemical performances associated with methanol oxidation on the Pt/MWCNT catalyst. **Figure 3** displays the results of line sweep voltammetry (LSV) analysis of MEOR on the Pt/MWCNT catalysts in an alkaline solution, executed at varying temperatures. At elevated temperature, the overall reaction rates experience significant acceleration compared to those observed at room temperature. The onset potential of methanol oxidation demonstrates a negative shift as temperature rises, indicating a reduced activity barrier for the reaction. Specifically, at 365 K, the onset potential of methanol oxidation on Pt/MWCNT catalysts is more than 120 mV negative compared to that observed at 298 K. Moreover, the peak current density at 363 K is approximately five times greater that recorded at 298 K (as detailed in **Table 1**).

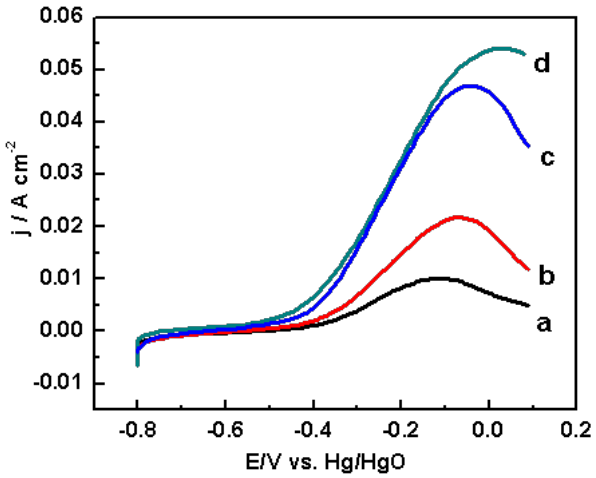

Figure 3. Line sweep of voltammgrams for oxidation of 1 mol/L methanol in 1 mol/L KOH (aq) on Pt/MWCNT electrode at different temperature (a: 298 K; b: 323 K; c: 343 K; d: 363 K). Scan rate: 50 mv/s

Table 1. Onset potential, peak current density, Tafel slope and exchange current density for methanol oxidation on Pt/MWCNT electrocatalyst

Temperature/K	Onset potential/V	Peak current density/mA	Tafel slope/mV·dec^{-1}	Exchange current density/mA·cm^{-2}
298	-0.40	36	138	0.028
323	-0.42	77	147	0.079
343	-0.48	165	172	0.178
363	-0.52	191	191	0.79

To delve into the kinetics of MEOR on Pt/MWCNT electrode across different temperatures, the interrelation of peak current density (derived from a forward scan) for methanol oxidation and the CV scan rate (v) was examined. The results of these investigations are illustrated in **Figure 4**.

Within the relatively low temperature range of 298-323 K, the observed trend in **Figure 4** unveils a proportionality between the peak current density and the square root of the scan rate. This observation indicates that the MEOR kinetics in this range may be governed by a diffusion process[23]. However, within the higher temperature span of 343 K to 363 K, a conspicuous deviation from this trend becomes apparent. This divergence suggests that the MEOR involves a surface process on the Pt/MWCNT catalysts in alkaline solution at higher temperature[24-26].

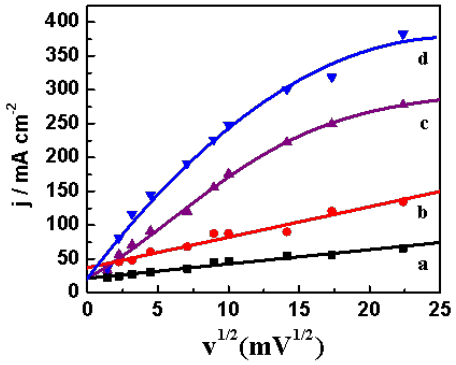

Figure 4. Peak current density *vs*. can rate ($v^{1/2}$) curves on Pt/MWCNT electrode in 1 mol/L KOH solution containing 1 mol/L CH_3OH at different temperature (a: 298 K; b: 323 K; c: 343 K; d: 363 K)

To further delve into the thermal kinetic attributes of MEOR on the Pt/MWCNT catalyst in an alkaline solution, Tafel slopes associated with MEOR were deduced from quasi-steady state polarization, as depicted in **Figure 5**. The obtained Tafel slopes, along with corresponding exchange current densities, have been extracted from the data in **Figure 5** and are listed in **Table 1**.

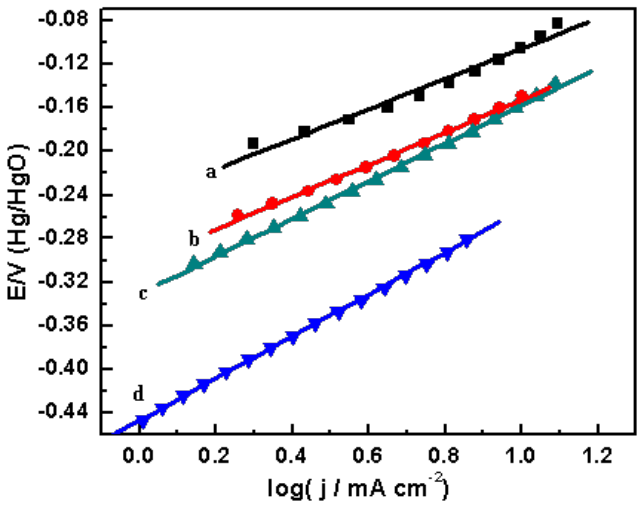

Figure 5. Tafel plots for methanol oxidation (1 mol/L CH_3OH) on the Pt/MWCNT electrode in 1 mol/L KOH solution at different temperatures (a: 298 K; b: 323 K; c: 343 K; d: 363 K). Scan rate: 5 mv/s

Specifically, the Tafel slopes obtained are approximately 110 mV/dec at 293 K and 114 mV/dec at 313 K for MEOR in alkaline solution. The values acquired through this study, across the entire temperature range, surpass those documented in existing literature[27-29]. As presented in **Table 1**, the Tafel slopes observed at 298 K and 323 K exhibit remarkable similarity, suggesting the presence of the same rate-determining step at both temperatures. A parallel observation is noted between 343 K and 363 K. However, with the temperature elevation from 323 K to 343 K, a noticeable rise in the Tafel slopes is evident, escalating from 147 mV/dec to 172 mV/dec. The variations in Tafel slope values can be attributed to alteration of the interphase condition, highlighting the impact of distinct rate-determining steps for the MEOR as a function of temperature[30-32].

Additionally. **Table 1** highlights that the exchange current density displays an upward trend corresponding to the increase in temperature. At 298 K, the curve was fitted with a single slope of approximately 138 mV/dec for the Pt/MWCNT, yielding an exchange current density of approximately 0.28×10^{-4} A/cm^2. Contrastingly, at 363 K, the Tafel slope measured around 191 mV/dec, accompanied by an exchange

current density of 0.79×10^{-3} A/cm^2. Remarkably, the exchange current density for the Pt/MWCNT electrode at 363 K surpassed that at 298 K by more than one order of magnitude.

3.4 Impedance Measurements

Figure 6 portrays Nyquist plots depicting the imaginary (Z''(Ω) versus real (Z' (Ω) component of the impedance for MEOR in an alkaline solution, observed across distinct potentials ranging from -0.5 V to 0.0 V *vs*. Hg/HgO at 298 K. Notably, At -0.5V, the impedance is subject to the influence of a sequence involving double layer charging, subsequently followed by the adsorption of methanol onto the electrode surface (observed in **Figure 6a**)[33]. The absence of a distinct semicircle in the Nyquist plot serves as corroborative evidence for this proposition. Notably, **Figure 6b-6e**, corresponding to electrode potentials within the range of -0.3 v ~ 0.0 V, shows well-defined semicircles. The emergence of semicircular patterns in the plots is indicative of reaction that are kinetically controlled[34]. These Nyquist plots provide insight into the electrode/electrolyte interface where the charge-transfer resistance prevails. Particularly, the semicircle observed at high frequencies which corresponds the charge transfer resistance (R) associated with the primary oxidation reaction, diminishes as the potential values shift towards a more positive direction[35]. **Figure 6f** exhibits a graphical representation of the charge transfer resistance (R) derived from the Nyquist plot in relation to the overpotential for the Pt/MWCNT electrode. The minimum value of R reflects the optimum condition of MEOR. The potential value serves as a driving force influencing MEOR kinetics. Conversely, the gradual increase of charge transfer resistance at elevated potential values can be interpreted as a results of surface obstruction caused by the by-products of MEOR[36].

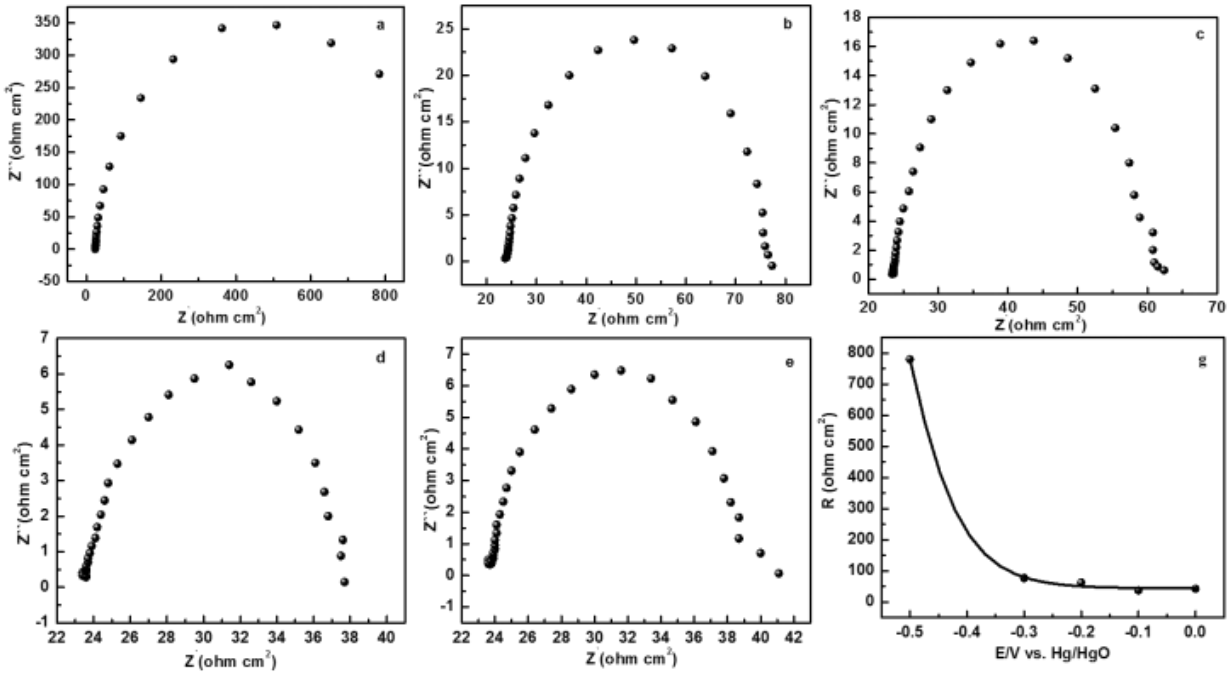

Figure 6. Nyquist plots of EIS for methanol oxidation on the Pt/MWCNT electrode in 1 mol/L KOH solution containing 1 mol/L CH_3OH at (a) -0.5 V; (b) -0.3 V; (c) -0.2 V; (d) -0.1 V; (e) 0.0 V and *vs*. Hg/HgO. The variation of the charge transfer resistance for Pt/MWCNT electrodes with potential (f)

Figure 7 showcases Nyquist plots depicting MEOR in alkaline solution, within temperature range from 323 K to 363 K. In contrast to the plots in **Figure 6**, the curves observed at higher temperatures deviate from regular semicircles. This deviation is attributed to the interplay between interfacial and diffusion impedances, as well as the roughness of the dispersed electrode surface with the temperature alteration[37].

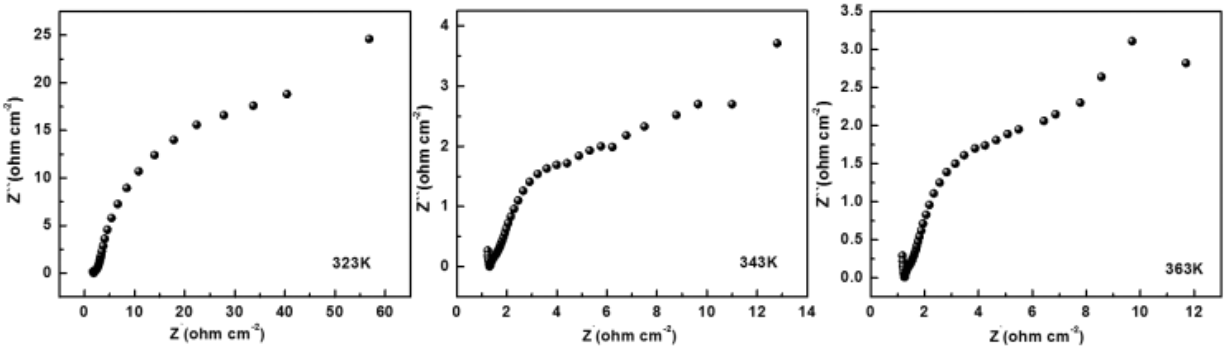

Figure 7. Nyquist plots of EIS for methanol oxidation on Pt/MWCNT electrodes in 1 mol/L KOH solution at different temperature

4. Conclusions

The oxidation of methanol was investigated on a Pt/MWCNT electrode in alkaline media within the temperature range of 298-363 K. The study employed cyclic voltammetry, quasi-state polarization, and electrochemical impedance spectroscopy methods to delve into the kinetics of the reaction.

It was observed that the onset potential of MEOR shifts towards more negative values with rising temperatures. This shift indicates a decreased activity barrier for the reaction. Specifically, at 363 K, the onset potential for methanol oxidation was 120 mV more negative compared to that at 298 K on the Pt/MWCNT electrode. Furthermore, the peak current density at 363 K was approximately five times higher than that at 298 K.

Tafel plots revealed that the rate-determining step of the MEOR varies with temperature changes. Additionally, the exchange current density showed an increase with higher temperatures. Especially, at 363 K, the exchange current density on the Pt/MWCNT electrode was more than one order of magnitude greater than at 298 K.

EIS results unveiled that the decline in charge-transfer resistance with increasing temperature could be attributed to the interplay between interfacial and diffusion impedances, alongside the surface roughness of the highly dispersed electrode surface.

Ethics Statement

Not applicable.

Consent for publication

Not applicable.

Availability of Supporting Data

Not applicable.

Conflict of Interest

We declare that the present work is approved for publication by all co-authors and the responsible authorities where the work was carried out.

Copyright

Reference

[1] Tiwari JN, Tiwari RN, Singh G, *et al*. Recent progress in the development of anode and cathode catalysts for direct methanol fuel cells. *Nano Energy*, 2013;2(5):553-578. https://doi.org/10.1016/j.nanoen.2013.06.009

[2] Gong L, Yang Z, Li K, *et al*. Recent development of methanol electrooxidation catalysts for direct methanol fuel cell. *Journal of Energy Chemistry*, 2018;27(6):1618-1628. https://doi.org/10.1016/j.jechem.2018.01.029

[3] Wang Y, Zou S and Cai WB. Recent advances on electro-oxidation of ethanol on Pt-and Pd-based *catalysts*: from reaction mechanisms to catalytic materials. Catalysts, 2015;5(3):1507-1534. https://doi.org/10.3390/catal5031507

[4] Zhao X, Liu Q, Li Q, *et al*. Two-dimensional electrocatalysts for alcohol oxidation: a critical review. *Chemical Engineering Journal*, 2020;400:125744. https://doi.org/10.1016/j.cej.2020.125744

[5] Chen W, Xue J, Bao Y, *et al*. Surface engineering of nano-ceria facet dependent coupling effect on

Pt nanocrystals for electro-catalysis of methanol oxidation reaction. *Chemical Engineering Journal*, 2020;381:122752. https://doi.org/10.1016/j.cej.2019.122752

[6] Zhang K, Wang H, Qiu J, *et al*. Multi-dimensional $Pt/Ni(OH)_2$/nitrogen-doped graphene nanocomposites with low platinum content for methanol oxidation reaction with highly catalytic performance. *Chemical Engineering Journal*, 2021;421:127786. https://doi.org/10.1016/j.cej.2020.127786

[7] Silva JCM, de Freitas IC, Neto AO, *et al*. Palladium nanoparticles supported on phosphorus-doped carbon for ethanol electro-oxidation in alkaline media. *Ionics*, 2018;24:1111-1119. https://doi.org/10.1007/s11581-017-2257-9

[8] Ning L, Liu X, Deng M, *et al*. Palladium-based nanocatalysts anchored on CNT with high activity and durability for ethanol electro-oxidation. *Electrochimica Acta*, 2019;297:206-214. https://doi.org/10.1016/j.electacta.2018.11.188

[9] Wang J, Sun H, Shah SA, *et al*. Palladium nanoparticles supported by three-dimensional freestanding electrodes for high-performance methanol electro-oxidation. *International Journal of Hydrogen Energy*, 2020;45(19):11089-11096. https://doi.org/10.1016/j.ijhydene.2020.02.046

[10] Tripković AV, Popović K D, Grgur BN, *et al*. Methanol electrooxidation on supported Pt and PtRu catalysts in acid and alkaline solutions. *Electrochimica Acta*, 2002;47(22-23):3707-3714. https://doi.org/10.1016/S0013-4686(02)00340-7

[11] Jayabal S, Saranya G, Geng D, *et al*. Insight into the correlation of Pt-support interactions with electrocatalytic activity and durability in fuel cells. *Journal of Materials Chemistry A*, 2020;8(19):9420-9446. https://doi.org/10.1039/D0TA01530J

[12] Zagoraiou E, Daletou MK, Sygellou L, *et al*. Highly dispersed platinum supported catalysts-effect of properties on the electrocatalytic activity. *Applied Catalysis B: Environmental*, 2019;259:118050. https://doi.org/10.1016/j.apcatb.2019.118050

[13] Yaqoob AA, Umar K and Ibrahim MNM. Silver nanoparticles: various methods of synthesis, size affecting factors and their potential applications-a review. Applied Nanoscience, 2020;10:1369-1378. https://doi.org/10.1007/s13204-020-01318-w

[14] Ortiz-Herrera JC, Cruz-Martínez H, Solorza-Feria O, *et al*. Recent progress in carbon nanotubes support materials for Pt-based cathode catalysts in PEM fuel cells. *International Journal of Hydrogen Energy*, 2022;47(70):30213-30224. https://doi.org/10.1016/j.ijhydene.2022.03.218

[15] Saha MS and Kundu A. Functionalizing carbon nanotubes for proton exchange membrane fuel cells electrode. *Journal of Power Sources*, 2010;195(19):6255-6261. https://doi.org/10.1016/j.jpowsour.2010.04.015

[16] Devrim Y and Arıca ED. Investigation of the effect of graphitized carbon nanotube catalyst support for high temperature PEM fuel cells. *International Journal of Hydrogen Energy*, 2020;45(5):3609-3617. https://doi.org/10.1016/j.ijhydene.2019.01.111

[17] Luo C, Xie H, Wang Q, *et al*. A review of the application and performance of carbon nanotubes in fuel cells. *Journal of Nanomaterials*, 2015;2015:4-4. https://doi.org/10.1155/2015/560392

[18] Hsieh CT, Gu J L, Tzou DY, *et al*. Microwave deposition of Pt catalysts on carbon nanotubes with different oxidation levels for formic acid oxidation. *International Journal of Hydrogen Energy*, 2013;38(25):10345-10353. https://doi.org/10.1016/j.ijhydene.2013.05.146

[19] Zhang W, Chen J, Swiegers GF, *et al*. *Microwave-assisted synthesis of Pt/CNT nanocomposite electrocatalysts for PEM fuel cells*. *Nanoscale*, 2010;2(2):282-286. https://doi.org/10.1039/B9NR00140A

[20] Xin Y, Liu J, Jie X, *et al*. Preparation and electrochemical characterization of nitrogen doped graphene by microwave as supporting materials for fuel cell catalysts. *Electrochimica Acta*, 2012;60:354-358. https://doi.org/10.1016/j.electacta.2011.11.062

[21] Bharti A, Cheruvally G and Muliankeezhu S. Microwave assisted, facile synthesis of Pt/CNT catalyst for proton exchange membrane fuel cell application. *International Journal of Hydrogen Energy*, 2017;42(16):11622-11631. https://doi.org/10.1016/j.ijhydene.2017.02.109

[22] Matseke MS, Munonde TS, Mallick K, *et al*. Pd/PANI/C nanocomposites as electrocatalysts for oxygen reduction reaction in alkaline media. *Electrocatalysis*, 2019;10:436-444. https://doi.org/10.1007/s12678-019-00536-3

[23] Gasteiger HA, Markovic N, Ross Jr PN, *et al*. Methanol electrooxidation on well-characterized platinum-ruthenium bulk alloys. *The Journal of Physical Chemistry*, 1993;97(46):12020-12029. https://doi.org/10.1021/j100148a030

[24] Li M, Wang Y, Cai J, *et al*. Surface sites assembled-strategy on Pt-Ru nanowires for accelerated methanol oxidation. *Dalton Transactions*, 2020;49(40):13999-14008. https://doi.org/10.1039/D0DT02567D

[25] Mekazni DS, Arán-Ais RM, Ferre-Vilaplana A, *et al*. Why methanol electro-oxidation on platinum in water takes place only in the presence of adsorbed OH. *ACS Catalysis*, 2022;12(3):1965-1970. https://doi.org/10.1021/acscatal.1c05122

[26] Díaz V, Ohanian M and Zinola CF. Kinetics of methanol electrooxidation on Pt/C and PtRu/C catalysts. *International Journal of Hydrogen Energy*, 2010;35(19):10539-10546. https://doi.org/10.1016/j.ijhydene.2010.07.135

[27] Zhang Y, Liu Y, Liu W, *et al*. Synthesis of honeycomb-like mesoporous nitrogen-doped carbon nanospheres as Pt catalyst supports for methanol oxidation in alkaline media. *Applied Surface Science*, 2017;407:64-71. https://doi.org/10.1016/j.apsusc.2017.02.158

[28] Jovanović VM, Terzić S, Tripković AV, *et al*. The effect of electrochemically treated glassy carbon on the activity of supported Pt catalyst in methanol oxidation. *Electrochemistry Communications*, 2004;6(12):1254-1258. https://doi.org/10.1016/j.elecom.2004.10.001

[29] Chen J, Wang M, Liu B, *et al*. Platinum catalysts prepared with functional carbon nanotube defects and its improved catalytic performance for methanol oxidation. *The Journal of Physical Chemistry B*, 2006;110(24):11775-11779. https://doi.org/10.1021/jp061045a

[30] Tripković AV, Popović KD, Lović JD, *et al*. Methanol oxidation at platinum electrodes in alkaline solution: comparison between supported catalysts and model systems. *Journal of Electroanalytical Chemistry*, 2004;572(1):119-128. https://doi.org/10.1016/j.jelechem.2004.06.007

[31] Kauranen PS, Skou E and Munk J. Kinetics of methanol oxidation on carbon-supported Pt and Pt+ Ru catalysts. *Journal of Electroanalytical Chemistry*, 1996;404(1):1-13. https://doi.org/10.1016/0022-0728(95)04298-9

[32] Iwasita T. Electrocatalysis of methanol oxidation. *Electrochimica Acta*, 2002;47(22-23):3663-3674. https://doi.org/10.1016/S0013-4686(02)00336-5

[33] Melnick RE and Palmore GTR. Impedance spectroscopy of the electro-oxidation of methanol on polished polycrystalline platinum. *The Journal of Physical Chemistry B*, 2001;105(5):1012-1025. https://doi.org/10.1021/jp0030847

[34] Cai GX, Guo JW, Wang J, *et al*. Negative resistance for methanol electro-oxidation on platinum/carbon (Pt/C) catalyst investigated by an electrochemical impedance spectroscopy. *Journal of Power Sources*, 2015;276:279-290. https://doi.org/10.1016/j.jpowsour.2014.11.131

[35] Jeon MK, Won JY, Oh KS, *et al*. Performance degradation study of a direct methanol fuel cell by electrochemical impedance spectroscopy. *Electrochimica Acta*, 2007;53(2):447-452. https://doi.org/10.1016/j.electacta.2007.06.063

[36] Wu G and Xu BQ. Carbon nanotube supported Pt electrodes for methanol oxidation: a comparison between multi-and single-walled carbon nanotubes. *Journal of Power Sources*, 2007;174(1):148-158. https://doi.org/10.1016/j.jpowsour.2007.08.024

[37] Mahapatra SS, Dutta A and Datta J. Temperature dependence on methanol oxidation and product formation on Pt and Pd modified Pt electrodes in alkaline medium. *International Journal of Hydrogen Energy*, 2011;36(22):14873-14883. https://doi.org/10.1016/j.ijhydene.2010.11.085